

## Article

# Biosynthesis of Xylariolide D in *Penicillium crustosum* Implies a Chain Branching Reaction Catalyzed by a Highly Reducing Polyketide Synthase

Sina A. Stierle and Shu-Ming Li \* 

Institut für Pharmazeutische Biologie und Biotechnologie, Fachbereich Pharmazie, Philipps-Universität Marburg, 35037 Marburg, Germany; sina.stierle@pharmazie.uni-marburg.de

\* Correspondence: shuming.li@staff.uni-marburg.de

**Abstract:** Fungi are important sources for the discovery of natural products. During the last decades, technological progress and the increasing number of sequenced genomes facilitated the exploration of new secondary metabolites. Among those, polyketides represent a structurally diverse group with manifold biological activities. In this study, we successfully used genome mining and genetic manipulation for functional proof of a polyketide biosynthetic gene cluster from the filamentous fungus *Penicillium crustosum*. Gene activation in the native host and heterologous expression in *Aspergillus nidulans* led to the identification of the *xil* cluster, being responsible for the formation of the 6-methyl-2-pyrone derivative xylariolide D. Feeding with <sup>13</sup>C-labeled precursors supported the hypothesis of chain branching during the backbone formation catalyzed by a highly reducing fungal polyketide synthase. A cytochrome P450-catalyzed hydroxylation converts the PKS product to the final metabolite. This proved that just two enzymes are required for the biosynthesis of xylariolide D.

**Keywords:** *Penicillium*; gene cluster; PKS; heterologous expression; xylariolide D

**Citation:** Stierle, S.A.; Li, S.-M.Biosynthesis of Xylariolide D in *Penicillium crustosum* Implies a Chain Branching Reaction Catalyzed by a Highly Reducing Polyketide Synthase. *J. Fungi* **2022**, *8*, 493. <https://doi.org/10.3390/jof8050493>

Academic Editor: Ulrich Kück

Received: 20 April 2022

Accepted: 6 May 2022

Published: 9 May 2022

**Publisher's Note:** MDPI stays neutral with regard to jurisdictional claims in published maps and institutional affiliations.



**Copyright:** © 2022 by the authors. Licensee MDPI, Basel, Switzerland. This article is an open access article distributed under the terms and conditions of the Creative Commons Attribution (CC BY) license (<https://creativecommons.org/licenses/by/4.0/>).

## 1. Introduction

Filamentous fungi, including *Penicillium* and *Aspergillus* species, are important sources for natural product (NP) discovery and drug development [1,2]. Polyketide NPs are structurally diverse secondary metabolites. Their backbones are assembled by polyketide synthases (PKSs) and often modified by different tailoring enzymes [3]. Type I fungal PKSs are iterative multifunctional enzymes that mainly use simple acyl building blocks to form a linear carbon chain [4]. In the first step, the PKS is primed with a starter unit, like acetyl-CoA, which is then condensed with an extender unit, e.g., malonyl-CoA. The C-C bond formation is catalyzed by the keto synthase (KS) domain via a decarboxylative Claisen condensation. To allow further chain elongation, the growing polyketide chain bound to the acyl carrier protein (ACP) is relocated to the KS domain. The acyltransferase (AT) domain is responsible for loading a new extender unit onto the ACP domain. Highly reducing (HR) PKSs consist of all reductive domains, i.e., dehydratase (DH), enoyl reductase (ER), and keto reductase (KR), which allow the optional full reduction of the  $\beta$ -keto group after Claisen condensation [4,5].

$\alpha$ -Carbon branches can be introduced into the backbone by methyltransferase (MT) domains using S-adenosyl methionine as the methyl donor or by extender units with  $\alpha$ -substituents like methylmalonyl-CoA [6]. Several enzymes that catalyze  $\beta$ -branching by condensation at the  $\beta$ -position to the carbonyl group of the ACP-bound polyketide chain have been reported, including RhiE with a B domain for the branching reaction [7,8].

*Penicillium crustosum* (*P. crustosum*) PRB-2 is a marine fungus isolated from deep-sea sediment [9]. Mining the genome of PRB-2 and gene prediction with antiSMASH [10] indicated the presence of at least 58 putative biosynthetic gene clusters for secondary metabolites. Previous work with *P. crustosum* PRB-2 revealed that only a few of these gene

clusters, such as those of peniphenones, penilactones, and their precursors, are expressed under laboratory conditions [11,12]. For uncovering NPs encoded by these silent or cryptic genes, gene activation in the producer and heterologous expression in a well-studied host have proven reliable genetic approaches [13,14], which were also successfully used for gene identification in PRB-2 [15]. To enhance genetic manipulation, a *pyrG* deficient strain FK15 was created in a previous study [16]. This strain was further modified by deletion of *pcr4870*, coding for the DNA repair protein subunit Ku70, to improve gene targeting efficiency. The resulting *P. crustosum*  $\Delta$ *pcr4870* $\Delta$ *pyrG* strain JZ02 can be conveniently used for gene deletion and activation experiments [17].

In this study, combined genetic approaches, including activation of genes in the native host as well as heterologous expression in *Aspergillus nidulans* (*A. nidulans*), were used to elucidate the function of a silent gene cluster from *P. crustosum* (Table S1). This led to the isolation of xylariolide D (**1**) and its congener prexylariolide D (**2**). Incorporation of <sup>13</sup>C-labeled precursors proved that the methyl residue of xylariolide D is derived from acetate, indicating that the highly reducing PKS also catalyzed a branching reaction during the biosynthesis.

## 2. Materials and Methods

### 2.1. Plasmids and Strains

Plasmids and strains used in this study are listed in Tables S2 and S3. All plasmids were constructed by using an assembly approach based on homologous recombination in *Saccharomyces cerevisiae* HOD114-2B [18]. For heterologous expression in *A. nidulans* LO8030 [19], an expression vector was created by using pJN17 as a template for the amplification of *Amp/URA3*, *wA* flanking regions, and *gpdA(p)* [20]. Instead of *AfriboB*, *AfpyrG* was amplified from the plasmid pYH-wA-pyrG [21] and used as a selection marker for all strains. The expression vector was sequenced to confirm correct assembly and linearized with *SfoI*. The genes for expression were amplified from genomic DNA (see Supplementary Materials for detail).

Plasmids for the activation of genes in the native host *P. crustosum* were assembled likewise: *Amp/URA3*, flanking regions, *AfpyrG*, *gpdA(p)*, and genes of interest were amplified by PCR and assembled via yeast homologous recombination. *E. coli* was used to amplify plasmids after construction in *S. cerevisiae* (see Supplementary Materials for more detail). Genetic manipulation in *E. coli* was carried out as described before [22].

### 2.2. Transformation of Fungal Strains and Confirmation of Integration

*A. nidulans* LO8030 and *P. crustosum* JZ02 were used for PEG-mediated protoplast transformation according to protocols described previously [12]. For selection of recombinant strains, media lacking uridine and uracil were used. Correct integration of the constructs into the genome was verified by PCR amplification with genomic DNA as template (see Supplementary Materials for more details). Afterward, transformants were cultivated, and the extracts were submitted to LC-MS analysis.

### 2.3. Cultivation of Fungal Strains, Extraction and Isolation of Secondary Metabolites

For LC-MS analysis, 50 mL of liquid glucose minimal medium [3] (GMM, see Supplementary Materials for more details) and Czapek-Dox (CD) medium were inoculated with spores and cultivated at 25 °C in the dark under static conditions. After 14 days, 1 mL of liquid culture was extracted with the same volume of EtOAc twice. After evaporation of the solvent, the residue was dissolved in 95% MeOH and submitted to LC-MS analysis (see Supplementary Materials for details).

Large-scale cultivation for the isolation of metabolites was carried out in 3 L GMM or Czapek-Dox (CD) medium. Compounds **1** and **2** were isolated from culture broths of *P. crustosum* SSt12, and compounds **2** and **3** were isolated from *A. nidulans* SSt04 and *A. nidulans* SSt26. After extraction with the same volume of EtOAc twice, the compounds were isolated

by silica gel chromatography and semi-preparative HPLC (see Supplementary Materials for details).

#### 2.4. Feeding with Prexylariolide D (2)

Cultivation was performed using 10 mL liquid GMM in 50 mL flasks at 25 °C in the dark under static conditions. Prexylariolide D (2) was dissolved in MeOH and added in a final concentration of 0.5 mM to 3-day-old cultures of *A. nidulans* SSt28 and *A. nidulans* LO8030. For LC-MS analysis, 0.5 mL samples were taken after 10 days of cultivation and extracted with the same volume of EtOAc.

#### 2.5. Incorporation of <sup>13</sup>C-Labeled Precursors

[2-<sup>13</sup>C] and [1,2-<sup>13</sup>C] acetate were purchased from Cambridge Isotope Laboratories, Inc. (Tewksbury, MA, USA). To isolate <sup>13</sup>C enriched 1 and 2 from *P. crustosum* SSt12, 2 × 250 mL of liquid GMM were inoculated with spores and kept at 25 °C for 3 days. For each flask, 75 mg of [2-<sup>13</sup>C] and [1,2-<sup>13</sup>C] acetate were dissolved in 1 mL of GMM and added to the cultures. Isolation was performed after 10 days of cultivation on a semi-preparative HPLC (see Supplementary Materials for more detail), leading to approximately 3 mg of analytically pure 1 and 2.

### 3. Results

#### 3.1. Bioinformatic Analysis

One of the putative silent clusters from *P. crustosum* PRB-2, termed the *xil* cluster in this study (Figure 1), attracted our attention. The cluster of interest comprises three genes coding for an HR-PKS XilA, a fungal-specific transcription factor XilB, and a cytochrome P450 enzyme XilC. BLAST search revealed that *xilA* and *xilC* share identical nucleotide sequences with those coding for KAF7517450.1 and KAF7517449.1 from *Penicillium crustosum* G10, respectively. An ortholog for *xilB* was not reported for strain G10. BLAST search also indicated the presence of a similar gene cluster in *Penicillium rubens* Wisconsin 54-1255 (=DSM 1075). XilA, XilB, and XilC show high sequence identities of 89.1, 85.8, and 93.0% to Pc16g04890, Pc16g04880, and Pc16g04870 from *P. rubens*, respectively (Figure 1) [23]. The polyketide synthases XilA and Pc16g04890 share the same domain structure comprising KS-AT-DH-MT-ER-KR-ACP with sequence identities from 82% to 96% on the amino acid level between the respective domains. In addition, XilA shows a sequence identity of 52.2% to the HR-PKS Sol1 (D7UQ44.1) from *Alternaria solani* with the same domain structure. This PKS assembles a 3-methyl-2-pyrone derivative as the PK scaffold [24–26].

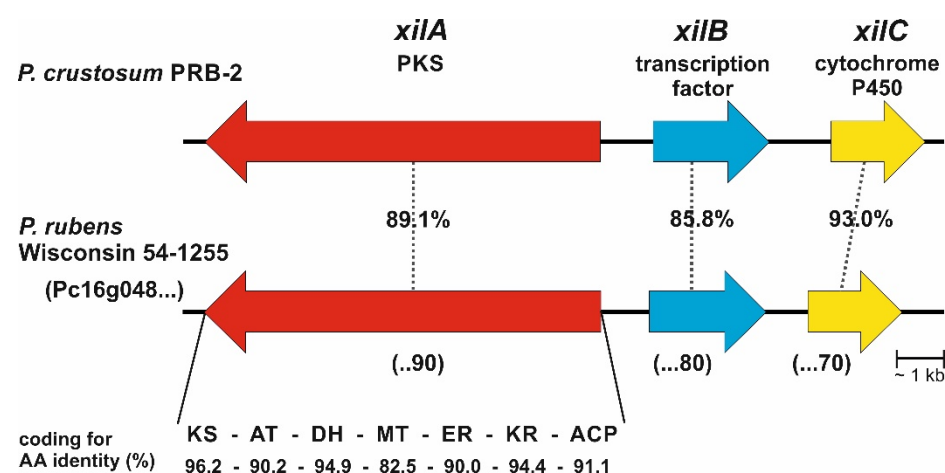


**Figure 1.** Comparison of *xil* cluster from *P. crustosum* PRB-2 with its ortholog from *P. rubens* Wisconsin 54-1255. Accession numbers for genes from *P. rubens* are given in parentheses.

### 3.2. Activation of Transcription Factor *xilB* and PKS *xilA* in *P. crustosum*

To identify the product of the *xil* cluster, we activated the transcription factor *xilB* by cloning the *gpdA(p)* promoter from *A. nidulans* [16] in front of its coding region. The resulting linearized construct pSSt02 was introduced into *P. crustosum* JZ02 via PEG-mediated protoplast transformation, as mentioned in Section 2.2. The obtained transformant *P. crustosum* SSt02 (*AfpyrG::gpdA(p)::xilB*) was verified via PCR (Figure S6) and cultivated in GMM for 14 days. In comparison to the control strain JZ02, LC-MS analysis revealed the presence of a new compound **1** with a  $[M+H]^+$  ion at  $m/z$  183.1019 in the extract of SSt02 (Figure 2A). However, the low quantity prohibited us from structure elucidation. Therefore, we used the same strategy as for *xilB* to activate the PKS gene *xilA*, resulting in strain *P. crustosum* SSt12 (*AfpyrG::gpdA(p)::xilA*). LC-MS analysis indicated an at least 17-fold higher accumulation of **1** in the *xilA* overexpression strain SSt12 than in the strain SSt02 after *xilB* activation (Figure 2A). Furthermore, another new compound **2** was detected with a  $[M+H]^+$  ion at  $m/z$  167.1067. Product yields of 27.5 and 12.9 mg/L were calculated for **1** and **2** in SSt12, respectively.

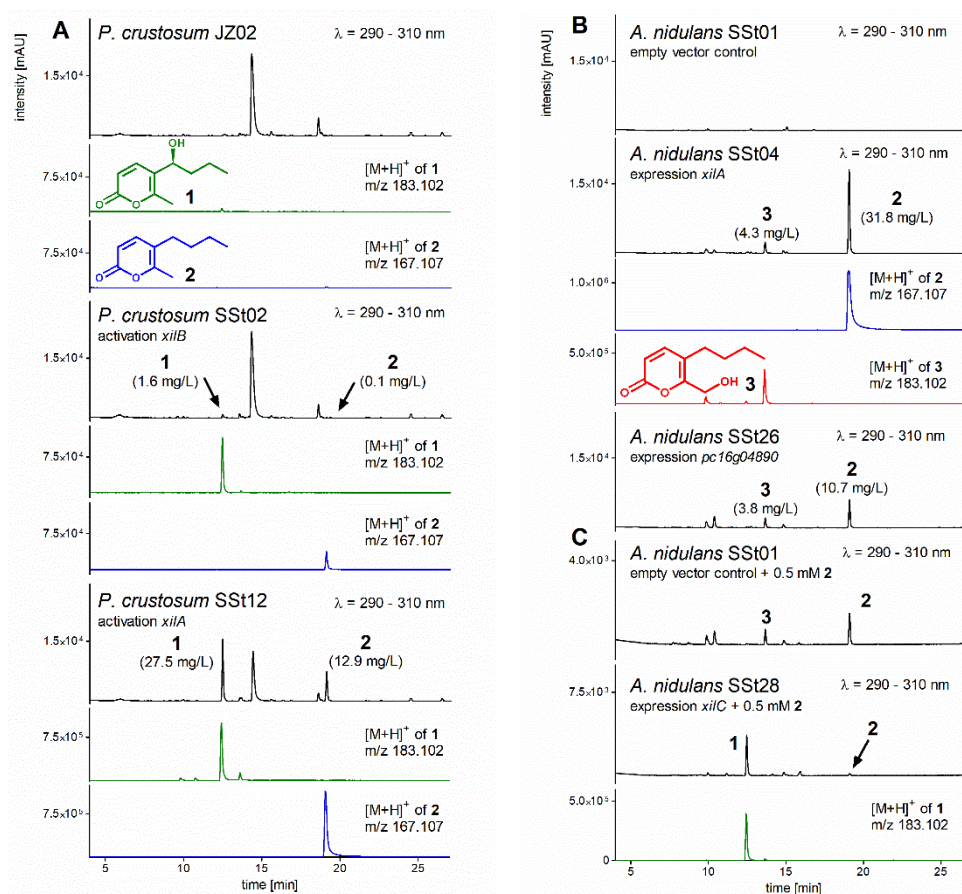


**Figure 2.** LC-MS analysis of fungal extracts. (A) Activation of the transcription factor *xilB* and polyketide synthase *xilA* in *P. crustosum*, (B) expression of *xilA* and its ortholog *pc16g04890* in *A. nidulans*, (C) adding **2** to *A. nidulans* with and without *xilC* expression. Compounds 1–3 with their EICs are highlighted in green, blue, and red, respectively. A tolerance range of  $\pm 0.005$  was used for ion detection. Product yields after gene activation or expression are given in parentheses under the compound numbers.

### 3.3. Heterologous Expression of *xilA* and *pc16g04890*

To identify the XilA product by heterologous expression in *A. nidulans*, *xilA* was cloned into the expression vector under the control of the constitutive *gpdA(p)* promoter and expressed in LO8030, resulting in the transformant *A. nidulans* SSt04. Compared to the

control strain *A. nidulans* SSt01, carrying the empty expression vector, SSt04 produced **2** and a new compound **3** with  $[M+H]^+$  ions at  $m/z$  167.1071 and 183.1016, respectively (Figure 2B). Compounds **1** and **3** share the same  $[M+H]^+$  ion but differ from each other in retention times. With a larger molecular mass of 16 daltons, they are likely hydroxylated products of **2**.

To confirm that the PKS Pc16g04890 from *P. rubens* Wisconsin 54-1255 produces the same compounds as XilA, its genomic sequence was also expressed in *A. nidulans*. Cultivation of the obtained transformant SSt26 led indeed to the accumulation of **2** and **3** (Figures 2B and S4).

### 3.4. Structure Elucidation

The obtained analytically pure compounds **1–3** were subjected to NMR analysis, including  $^1\text{H-NMR}$ ,  $^{13}\text{C-NMR}$ , HMBC, and HSQC (Figures S7–S20). Interpretation of the NMR spectra and comparison with data in the literature proved **1** and **2** to be xylariolide D [27] and its non-hydroxylated precursor 5-butyl-6-methyl-2H-pyran-2-one (named prexylariolide D in this study) [28], respectively (see Figures 2 and 3 for structures). ECD spectrum (Figure S23) confirmed the S-configuration of **1**, as reported previously [27]. It can be speculated that **2** is the PKS (XilA) product and hydroxylated to **1** by the cytochrome P450 enzyme XilC in *P. crustosum* (Figure 4). Comparison of the NMR data of **2** and **3** revealed that the signals at  $\delta_{\text{H}}$  2.22 (s, 3H) and  $\delta_{\text{C}}$  17.2 ppm for the methyl group at the 2-pyrone ring of **2** disappeared in the spectra of **3**. Instead, signals for a methylene group were observed at  $\delta_{\text{H}}$  4.45 (s, 2H) and  $\delta_{\text{C}}$  59.0 ppm (Figures S12, S13, S16, and S17), indicating the conversion of the methyl to a hydroxymethyl group in **3**. This was also confirmed by HSQC and HMBC analyses. Since **3** (named xylariolide G) is not produced by the native host *P. crustosum*, even after activation of *xilA* or *xilB*, we assume that the conversion of **2** to **3** in *A. nidulans* SSt04 is catalyzed by an enzyme from the host strain, as observed for a methylated isocoumarin after heterologous expression of a PKS gene [22].

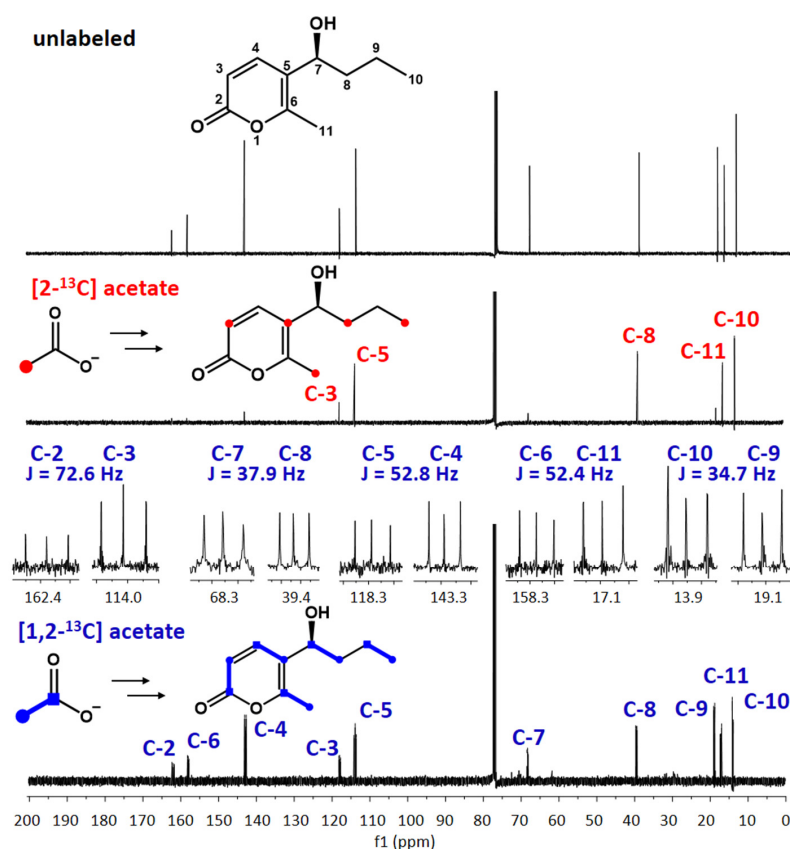


Figure 3.  $^{13}\text{C-NMR}$  spectra of xylariolide D (**1**) without and with  $^{13}\text{C}$ -labeled acetate.



of other systems like the global regulation of secondary metabolism. Furthermore, the production of both compounds **1** and **2** in *P. crustosum* SSt12 after overexpression of *xilA* indicates that the formation of the polyketide scaffold, and not the hydroxylation, is the limiting step in the biosynthesis of xylariolide D.

As shown in Figure 2, feeding of prexylariolide D (**2**) led to the accumulation of xylariolide D (**1**) in the *xilC* overexpression strain *A. nidulans* SSt28 and xylariolide G (**3**) in the control *A. nidulans* SSt01. Dihydroxylated derivative was not detected in SSt28, proving the higher substrate specificity of XilC toward its natural substrate **2** than the unknown hydroxylase from *A. nidulans*. Only in the absence of XilC, prexylariolide D (**2**) was converted to **3** by the hydroxylase from *A. nidulans*.

## 5. Conclusions

In conclusion, we elucidated the function of a silent gene cluster for the biosynthesis of xylariolide D (**1**) in two fungal strains by gene activation in the native strain and heterologous expression in a well-studied host. Activation of the PKS gene *xilA* led to the accumulation of **1** with a much higher yield than the activation of the putative transcription factor *xilB*. Feeding experiments confirmed that XilC catalyzes the hydroxylation of prexylariolide D (**2**) to **1**. The incorporation of <sup>13</sup>C-labeled precursors provides clear evidence for acetate as the origin of the methyl group at the 2-pyrone ring. Further investigation, such as the biochemical characterization or elucidation of the XilA structure, will gain deeper insight into the unusual formation of the 5-alkyl-6-methyl-2-pyrone backbone.

**Supplementary Materials:** The following supporting information can be downloaded at: <https://www.mdpi.com/article/10.3390/jof8050493/s1>. Table S1. *xil* cluster in *P. crustosum* and *P. rubens*. Table S2. Strains used in this study. Table S3. Oligonucleotide primers and plasmids used in this study. Table S4. NMR data of compounds **1**, **2** and **3** in CDCl<sub>3</sub>. Table S5. Enrichments and coupling constants in **1** and **2** after feeding with <sup>13</sup>C labeled precursors. Figure S1. Schematic representation of plasmid creation. Figure S2. Schematic representation of gene integration into the *wA* PKS locus of *A. nidulans* LO8030. Figure S3. Verification of plasmid pSSt04 and correct integration in *A. nidulans* SSt04 transformants. Figure S4. Verification of plasmid pSSt26 and correct integration in *A. nidulans* SSt26 transformant. Figure S5. Verification of plasmid pSSt28 and correct integration in *A. nidulans* SSt28 transformants. Figure S6. Verification of plasmids and correct gene integration in *P. crustosum* transformants. Figure S7. <sup>1</sup>H-NMR of compound **1** in CDCl<sub>3</sub> (500 MHz). Figure S8. <sup>13</sup>C-NMR of compound **1** in CDCl<sub>3</sub> (125 MHz). Figure S9. HSQC of compound **1** in CDCl<sub>3</sub>. Figure S10. HMBC of compound **1** in CDCl<sub>3</sub>. Figure S11. H,H-COSY of compound **1** in CDCl<sub>3</sub>. Figure S12. <sup>1</sup>H-NMR of compound **2** in CDCl<sub>3</sub> (500 MHz). Figure S13. <sup>13</sup>C-NMR of compound **2** in CDCl<sub>3</sub> (125 MHz). Figure S14. HSQC of compound **2** in CDCl<sub>3</sub>. Figure S15. HMBC of compound **2** in CDCl<sub>3</sub>. Figure S16. <sup>1</sup>H-NMR of compound **3** in CDCl<sub>3</sub> (500 MHz). Figure S17. <sup>13</sup>C-NMR of compound **3** in CDCl<sub>3</sub> (125 MHz). Figure S18. HSQC of compound **3** in CDCl<sub>3</sub>. Figure S19. HMBC of compound **3** in CDCl<sub>3</sub>. Figure S20. H,H-COSY of compound **3** in CDCl<sub>3</sub>. Figure S21. <sup>13</sup>C-NMR of compound **2** in CDCl<sub>3</sub>, enriched with [2-<sup>13</sup>C] acetate (125 MHz). Figure S22. <sup>13</sup>C-NMR of compound **2** in CDCl<sub>3</sub>, enriched with [1,2-<sup>13</sup>C] acetate (125 MHz). Figure S23. ECD-spectrum of compound **1** (0.7 mg/mL) in MeOH. Ref. [32] is cited in Supplementary Materials.

**Author Contributions:** Conceptualization, S.A.S. and S.-M.L.; bioinformatics and experiments, S.A.S.; data analysis, S.A.S. and S.-M.L. writing—original draft preparation, S.A.S.; writing—review and editing, S.A.S. and S.-M.L.; supervision, S.-M.L.; project administration, S.-M.L.; funding acquisition, S.-M.L. All authors have read and agreed to the published version of the manuscript.

**Funding:** This research was financially funded in part by the DFG (INST 160/620-1 and Li844/11-1 to S.-M.L.).

**Institutional Review Board Statement:** Not applicable.

**Informed Consent Statement:** Not applicable.

**Data Availability Statement:** Not applicable.

**Acknowledgments:** We thank L. Ludwig-Radtke, R. Kraut, and S. Newel for LC-MS and NMR analyses.

**Conflicts of Interest:** The authors declare no conflict of interest. The funders had no role in the design of the study, in the collection, analyses, or interpretation of data; in the writing of the manuscript; or in the decision to publish the results.

## References

1. Hoffmeister, D.; Keller, N.P. Natural products of filamentous fungi: Enzymes, genes, and their regulation. *Nat. Prod. Rep.* **2007**, *24*, 393. [[CrossRef](#)] [[PubMed](#)]
2. Newman, D.J.; Cragg, G.M. Natural products as sources of new drugs over the nearly four decades from 01/1981 to 09/2019. *J. Nat. Prod.* **2020**, *83*, 770. [[CrossRef](#)] [[PubMed](#)]
3. Keller, N.P. Fungal secondary metabolism: Regulation, function and drug discovery. *Nat. Rev. Microbiol.* **2019**, *17*, 167. [[CrossRef](#)] [[PubMed](#)]
4. Cox, R.J. Polyketides, proteins and genes in fungi: Programmed nano-machines begin to reveal their secrets. *Org. Biomol. Chem.* **2007**, *5*, 2010. [[CrossRef](#)]
5. Cox, R.J.; Simpson, T.J. Fungal type I polyketide synthases. *Methods Enzymol.* **2009**, *459*, 49.
6. Yang, X.L.; Friedrich, S.; Yin, S.; Piech, O.; Williams, K.; Simpson, T.J.; Cox, R.J. Molecular basis of methylation and chain-length programming in a fungal iterative highly reducing polyketide synthase. *Chem. Sci.* **2019**, *10*, 8478. [[CrossRef](#)]
7. Walker, P.D.; Weir, A.N.M.; Willis, C.L.; Crump, M.P. Polyketide  $\beta$ -branching: Diversity, mechanism and selectivity. *Nat. Prod. Rep.* **2021**, *38*, 723–756. [[CrossRef](#)]
8. Bretschneider, T.; Heim, J.B.; Heine, D.; Winkler, R.; Busch, B.; Kusebauch, B.; Stehle, T.; Zocher, G.; Hertweck, C. Vinylogous chain branching catalysed by a dedicated polyketide synthase module. *Nature* **2013**, *502*, 124. [[CrossRef](#)]
9. Wu, G.; Ma, H.; Zhu, T.; Li, J.; Gu, Q.; Li, D. Penilactones A and B, two novel polyketides from Antarctic deep-sea derived fungus *Penicillium crustosum* PRB-2. *Tetrahedron* **2012**, *68*, 9745. [[CrossRef](#)]
10. Blin, K.; Shaw, S.; Kloosterman, A.M.; Charlop-Powers, Z.; Van Wezel, G.P.; Medema, M.H.; Weber, T. antiSMASH 6.0: Improving cluster detection and comparison capabilities. *Nucleic Acids Res.* **2021**, *49*, W29. [[CrossRef](#)]
11. Fan, J.; Liao, G.; Ludwig-Radtke, L.; Yin, W.-B.; Li, S.-M. Formation of terrestrial acid in *Penicillium crustosum* requires redox-assisted decarboxylation and stereoisomerization. *Org. Lett.* **2020**, *22*, 88. [[CrossRef](#)] [[PubMed](#)]
12. Fan, J.; Liao, G.; Kindinger, F.; Ludwig-Radtke, L.; Yin, W.-B.; Li, S.-M. Peniphenone and penilactone formation in *Penicillium crustosum* via 1,4-Michael additions of *ortho*-quinone methide from hydroxyclovatol to  $\gamma$ -butyrolactones from crustosic acid. *J. Am. Chem. Soc.* **2019**, *141*, 4225. [[CrossRef](#)] [[PubMed](#)]
13. Scherlach, K.; Hertweck, C. Mining and unearthing hidden biosynthetic potential. *Nat. Commun.* **2021**, *12*, 3864. [[CrossRef](#)] [[PubMed](#)]
14. Medema, M.H.; de Rond, T.; Moore, B.S. Mining genomes to illuminate the specialized chemistry of life. *Nat. Rev. Genet.* **2021**, *22*, 553. [[CrossRef](#)] [[PubMed](#)]
15. Xiang, P.; Li, S.-M. Formation of 3-orsellinoxipropanoic acid in *Penicillium crustosum* is catalyzed by a bifunctional nonreducing polyketide synthase. *Org. Lett.* **2022**, *24*, 462. [[CrossRef](#)] [[PubMed](#)]
16. Kindinger, F.; Nies, J.; Becker, A.; Zhu, T.; Li, S.-M. Genomic locus of a *Penicillium crustosum* pigment as an integration site for secondary metabolite gene expression. *ACS Chem. Biol.* **2019**, *14*, 1227. [[CrossRef](#)]
17. Zhou, J.; Li, S.-M. Conversion of viridicatic acid to crustosic acid by cytochrome P450 enzyme-catalysed hydroxylation and spontaneous cyclisation. *App. Microbiol. Biotechnol.* **2021**, *105*, 9181. [[CrossRef](#)]
18. Mojardín, L.; Vega, M.; Moreno, F.; Schmitz, H.P.; Heinisch, J.J.; Rodicio, R. Lack of the NAD<sup>+</sup>-dependent glycerol 3-phosphate dehydrogenase impairs the function of transcription factors Sip4 and Cat8 required for ethanol utilization in *Kluyveromyces lactis*. *Fungal. Genet. Biol.* **2018**, *111*, 16. [[CrossRef](#)]
19. Chiang, Y.M.; Ahuja, M.; Oakley, C.E.; Entwistle, R.; Asokan, A.; Zutz, C.; Wang, C.C.; Oakley, B.R. Development of genetic dereplication strains in *Aspergillus nidulans* results in the discovery of aspercryptin. *Angew. Chem. Int. Ed. Engl.* **2016**, *55*, 1662. [[CrossRef](#)]
20. Nies, J.; Li, S.-M. Prenylation and dehydrogenation of a C2-reversely prenylated diketopiperazine as a branching point in the biosynthesis of echinulin family alkaloids in *Aspergillus ruber*. *ACS Chem. Biol.* **2021**, *16*, 185. [[CrossRef](#)]
21. Yin, W.B.; Chooi, Y.H.; Smith, A.R.; Cacho, R.A.; Hu, Y.; White, T.C.; Tang, Y. Discovery of cryptic polyketide metabolites from dermatophytes using heterologous expression in *Aspergillus nidulans*. *ACS Synth. Biol.* **2013**, *2*, 629. [[CrossRef](#)] [[PubMed](#)]
22. Xiang, P.; Ludwig-Radtke, L.; Yin, W.-B.; Li, S.-M. Isocoumarin formation by heterologous gene expression and modification by host enzymes. *Org. Biomol. Chem.* **2020**, *18*, 4946. [[CrossRef](#)] [[PubMed](#)]
23. Guzman-Chavez, F.; Zwahlen, R.D.; Bovenberg, R.A.L.; Driessen, A.J.M. Engineering of the filamentous fungus *Penicillium chrysogenum* as cell factory for natural products. *Front. Microbiol.* **2018**, *9*, 2768. [[CrossRef](#)] [[PubMed](#)]
24. Katayama, K.; Kobayashi, T.; Oikawa, H.; Honma, M.; Ichihara, A. Enzymatic activity and partial purification of solanapyrone synthase: First enzyme catalyzing Diels-Alder reaction. *Biochim. Biophys. Acta* **1998**, *1384*, 387. [[CrossRef](#)]
25. Katayama, K.; Kobayashi, T.; Chijimatsu, M.; Ichihara, A.; Oikawa, H. Purification and N-terminal amino acid sequence of solanapyrone synthase, a natural Diels-Alderase from *Alternaria solani*. *Biosci. Biotechnol. Biochem.* **2008**, *72*, 604. [[CrossRef](#)]

26. Kasahara, K.; Miyamoto, T.; Fujimoto, T.; Oguri, H.; Tokiwano, T.; Oikawa, H.; Ebizuka, Y.; Fujii, I. Solanapyrone synthase, a possible Diels-Alderase and iterative type I polyketide synthase encoded in a biosynthetic gene cluster from *Alternaria solani*. *ChemBiochem* **2010**, *11*, 1245. [[CrossRef](#)]
27. Liu, C.C.; Zhang, Z.Z.; Feng, Y.Y.; Gu, Q.Q.; Li, D.H.; Zhu, T.J. Secondary metabolites from Antarctic marine-derived fungus *Penicillium crustosum* HDN153086. *Nat. Prod. Res.* **2019**, *33*, 414. [[CrossRef](#)]
28. Schlingmann, G.; Milne, L.; Carter, G.T. New  $\alpha$ -pyrones produced by fungal culture LL-11G219 function as androgen receptor ligands. *Tetrahedron* **1998**, *54*, 13013. [[CrossRef](#)]
29. Hu, Z.-Y.; Li, Y.-Y.; Lu, C.-H.; Lin, T.; Hu, P.; Shen, Y.-M. Seven novel linear polyketides from *Xylaria* sp. NCY2. *Helv. Chim. Acta* **2010**, *93*, 925. [[CrossRef](#)]
30. Cadelis, M.M.; Gordon, H.; Grey, A.; Geese, S.; Mulholland, D.R.; Weir, B.S.; Copp, B.R.; Wiles, S. Isolation of a novel polyketide from *Neodidymelliopsis* sp. *Molecules* **2021**, *26*, 3235. [[CrossRef](#)]
31. Tran, T.D.; Wilson, B.A.P.; Henrich, C.J.; Wendt, K.L.; King, J.; Cichewicz, R.H.; Stchigel, A.M.; Miller, A.N.; O'Keefe, B.R.; Gustafson, K.R. Structure elucidation and absolute configuration of metabolites from the soil-derived fungus *Dictyosporium digitatum* using spectroscopic and computational methods. *Phytochemistry* **2020**, *173*, 112278. [[CrossRef](#)] [[PubMed](#)]
32. Watanabe, A.; Fujii, I.; Sankawa, U.; Mayorga, M.E.; Timberlake, W.E.; Ebizuka, Y. Reidentification of *Aspergillus nidulans* wA gene to code for a polyketide synthase of naphthopyrone. *Tetrahedron Lett.* **1999**, *40*, 91. [[CrossRef](#)]